Generalized Digital Waveguide Networks

Davide Rocchesso, Julius O. Smith III

Abstract— **Digital waveguides are generalized to the multivariable case with the goal of maximizing generality while retaining robust numerical properties and simplicity of realization. Multivariable complex power is defined, and conditions for "medium passivity" are presented. Multivariable complex wave impedances, such as those deriving from multivariable lossy waveguides, are used to construct scattering junctions which yield frequency dependent scattering coefficients which can be implemented in practice using digital filters. The general form for the scattering matrix at a junction of multivariable waveguides is derived. An efficient class of loss-modeling filters is derived, including a rule for checking validity of the small-loss assumption. An example application in musical acoustics is given.**

I. INTRODUCTION

Digital Waveguide Networks (DWN) have been widely used to develop efficient discrete-time physical models for sound synthesis, particularly for woodwind, string, and brass musical instruments [1], [2], [3], [4], [5], [6], [7]. They were initially developed for artificial reverberation [8], [9], [10], and more recently they have been applied to robust numerical simulation of 2D and 3D vibrating systems [11], [12], [13], [14], [15], [16], [17].

A digital waveguide may be thought of as a sampled transmission line—or acoustic waveguide—in which sampled, unidirectional traveling waves are explicitly simulated. Simulating traveling-wave components in place of physical variables such as pressure and velocity can lead to significant computational reductions, particularly in sound synthesis applications, since the models for most traditional musical instruments (in the string, wind, and brass families), can be efficiently simulated using one or two long delay lines together with sparsely distributed scattering junctions and filters [2], [18], [19]. Moreover, desirable numerical properties are more easily ensured in this framework, such as stability [20], "passivity" of round-off errors, and minimized sensitivity to coeffi-

D. Rocchesso is with the Dipartimento di Informatica, Università degli Studi di Verona, strada Le Grazie, 37134 Verona - ITALY, Phone: ++39.045.8027979, FAX: ++39.045.8027982, E-mail: rocchesso@sci.univr.it. J. O. Smith is with the Center for Computer Research in Music and Acoustics (CCRMA), Music Department, Stanford University, Stanford, CA 94305, E-mail: jos@ccrma.stanford.edu.

cient quantization [21], [22], [23], [14].

In [24], a multivariable formulation of digital waveguides was proposed in which the real, positive, characteristic impedance of the waveguide medium (be it an electric transmission line or an acoustic tube) is generalized to any $q \times q$ para-Hermitian matrix. The associated wave variables were generalized to a $q \times m$ matrix of z transforms. From fundamental constraints assumed at a junction of two or more waveguides (pressure continuity, conservation of flow), associated multivariable scattering relations were derived, and various properties were noted.

In this paper, partially based on [25], we pursue a different path to vectorized DWNs, starting with a multivariable generalization of the well known *telegrapher's equations* [26]. This formulation provides a more detailed physical interpretation of generalized quantities, and new potential applications are indicated.

The paper is organized as follows. Section II introduces the generalized DWN formulation, starting with the scalar case and proceeding to the multivariable case. The generalized wave impedance and complex signal power appropriate to this formulation are derived, and conditions for "passive" computation are given. In Section III, *losses* are introduced, and some example applications are considered. Finally, Section IV presents a derivation of the general form of the physical scattering junctions induced intersecting multivariable digital waveguides.

II. MULTIVARIABLE DWN FORMULATION

This section reviews the DWN paradigm and briefly outlines considerations arising in acoustic simulation applications. The multivariable formulation is based on m-dimensional vectors of "pressure" and "velocity" $\boldsymbol{p}$ and $\boldsymbol{u}$, respectively. These variables can be associated with physical quantities such as acoustic pressure and velocity, respectively, or they can be anything analogous such as electrical voltage and current, or mechanical force and velocity. We call these dual variables *Kirchhoff variables* to distinguish them from *wave variables* [22] which are their traveling-wave components. In other words, in a 1D waveguide, two components traveling in opposite directions must

be summed to produce a physical variable. For concreteness, we will focus on generalized pressure and velocity waves in a lossless, linear, *acoustic tube*. In acoustic tubes, velocity waves are in units of volume velocity (particle velocity times cross-sectional area of the tube) [27].

A. The Ideal Waveguide

First we address the scalar case. For an ideal acoustic tube, we have the following *wave equation* [27]:

$$\frac{\partial^2 p(x,t)}{\partial t^2} = c^2 \frac{\partial^2 p(x,t)}{\partial x^2}, \tag{1}$$

where $p(x,t)$ denotes (scalar) pressure in the tube at the point x along the tube at time t in seconds. If the length of the tube is L_R, then x is taken to lie between 0 and L_R. We adopt the convention that x increases "to the right" so that waves traveling in the direction of increasing x are referred to as "right-going." The constant c is the speed of sound propagation in the tube, given by $c = \sqrt{K/\mu}$, where K is the "tension[1]" of the gas in the tube, and μ is the mass per unit volume of the tube. The dual variable, volume velocity u, also obeys (1) with p replaced by u. The wave equation (1) also holds for an ideal string, if p represents the transverse displacement, K is the tension of the string, and μ is its linear mass density.

The wave equation (1) follows from the more physically meaningful equations [28, p. 243]:

$$-\frac{\partial p(x,t)}{\partial x} = \mu \frac{\partial u(x,t)}{\partial t} \tag{2}$$

$$-\frac{\partial u(x,t)}{\partial x} = K^{-1}\frac{\partial p(x,t)}{\partial t}. \tag{3}$$

Equation (2) follows immediately from Newton's second law of motion, while (3) follows from conservation of mass and properties of an ideal gas.

The general traveling-wave solution to (1), or (2) and (3), was given by D'Alembert as [27]

$$\begin{aligned} p(x,t) &= p^+(x-ct) + p^-(x+ct) \\ u(x,t) &= u^+(x-ct) + u^-(x+ct), \end{aligned} \tag{4}$$

where p^+, p^-, u^+, u^- are the right- and left-going wave components of pressure and velocity, respectively, and are referred to as *wave variables*. This solution form is interpreted as the sum of two fixed

---

[1] "Tension" is defined here for gases as the reciprocal of the adiabatic compressibility of the gas [28, p. 230]. This definition helps to unify the scattering formalism for acoustic tubes with that of mechanical systems such as vibrating strings.

wave-shapes traveling in opposite directions along the tube. The specific waveshapes are determined by the initial pressure $p(x,0)$ and velocity $u(x,0)$ throughout the tube $x \in [0, L_R]$.

B. Multivariable Formulation of the Waveguide

Perhaps the most straightforward multivariable generalization of (2) and (3) is

$$\frac{\partial \boldsymbol{p}(\boldsymbol{x},t)}{\partial \boldsymbol{x}} = -\boldsymbol{M}\frac{\partial \boldsymbol{u}(\boldsymbol{x},t)}{\partial t} \tag{5}$$

$$\frac{\partial \boldsymbol{p}(\boldsymbol{x},t)}{\partial t} = -\boldsymbol{K}\frac{\partial \boldsymbol{u}(\boldsymbol{x},t)}{\partial \boldsymbol{x}} \tag{6}$$

in the spatial coordinates $\boldsymbol{x}^T \triangleq [x_1 \cdots x_m]$ at time t, where $\boldsymbol{M}$ and $\boldsymbol{K}$ are $m \times m$ non-singular matrices playing the respective roles of multidimensional mass and tension. Differentiating (5) with respect to $\boldsymbol{x}$ and (6) with respect to t, and eliminating the term $\partial^2 \boldsymbol{u}(\boldsymbol{x},t)/\partial \boldsymbol{x}\partial t$ yields the m-variable generalization of the wave equation

$$\frac{\partial^2 \boldsymbol{p}(\boldsymbol{x},t)}{\partial t^2} = \boldsymbol{K}\boldsymbol{M}^{-1}\frac{\partial^2 \boldsymbol{p}(\boldsymbol{x},t)}{\partial \boldsymbol{x}^2}. \tag{7}$$

The second spatial derivative is defined here as

$$\left[\frac{\partial^2 \boldsymbol{p}(\boldsymbol{x},t)}{\partial \boldsymbol{x}^2}\right]^T \triangleq \left[\begin{array}{ccc} \frac{\partial^2 p_1(\boldsymbol{x},t)}{\partial x_1^2} & \cdots & \frac{\partial^2 p_m(\boldsymbol{x},t)}{\partial x_m^2} \end{array}\right]. \tag{8}$$

Similarly, differentiating (5) with respect to t and (6) with respect to $\boldsymbol{x}$, and eliminating $\partial^2 \boldsymbol{p}(\boldsymbol{x},t)/\partial \boldsymbol{x}\partial t$ yields

$$\frac{\partial^2 \boldsymbol{u}(\boldsymbol{x},t)}{\partial t^2} = \boldsymbol{M}^{-1}\boldsymbol{K}\frac{\partial^2 \boldsymbol{u}(\boldsymbol{x},t)}{\partial \boldsymbol{x}^2}. \tag{9}$$

For digital waveguide modeling, we desire solutions of the multivariable wave equation involving only sums of traveling waves. Consider the eigenfunction

$$\boldsymbol{p}(\boldsymbol{x},t) = \left[\begin{array}{c} e^{st+v_1 x_1} \\ \ldots \\ e^{st+v_m x_m} \end{array}\right] \triangleq e^{st\boldsymbol{I}+\boldsymbol{V}\boldsymbol{X}} \cdot \boldsymbol{1}, \tag{10}$$

where s is interpreted as a Laplace-transform variable $s = \sigma + j\omega$, $\boldsymbol{I}$ is the $m \times m$ identity matrix, $\boldsymbol{X} \triangleq \text{diag}(\boldsymbol{x})$, $\boldsymbol{V} \triangleq \text{diag}([v_1, \ldots, v_m])$ is a diagonal matrix of spatial Laplace-transform variables (the imaginary part of v_i being spatial frequency along the ith spatial coordinate), and $\boldsymbol{1}^T \triangleq [1, \ldots, 1]$ is the m-dimensional vector of ones. Applying the eigenfunction (10) to (7) gives the algebraic equation

$$s^2 \boldsymbol{I} = \boldsymbol{K}\boldsymbol{M}^{-1}\boldsymbol{V}^2 \triangleq \boldsymbol{C_p}^2 \boldsymbol{V}^2, \tag{11}$$

where C_p is the diagonal matrix of sound-speeds along the m coordinate axes. Since $C_p{}^2 V^2 = s^2 I$, we have

$$V = \pm s C_p{}^{-1} . \tag{12}$$

Substituting (12) into (10), the eigensolutions of (7) are found to be of the form

$$p(x,t) = e^{s\left(tI \pm C_p{}^{-1} X\right)} \cdot \mathbf{1} . \tag{13}$$

Similarly, applying (10) to (9) yields

$$V = \pm s C_u{}^{-1} , \tag{14}$$

where $C_u \overset{\triangle}{=} M^{-1} K$. The eigensolutions of (9) are then of the form

$$u(x,t) = e^{s\left(tI \pm C_u{}^{-1} X\right)} \cdot \mathbf{1} . \tag{15}$$

The generalized sound-speed matrices C_p and C_u are the same whenever M^{-1} and K *commute*, e.g., when they are both diagonal.

Having established that (13) is a solution of (7) when condition (11) holds on the matrices M and K, we can express the general traveling-wave solution to (7) in both pressure and velocity as

$$\begin{aligned} p(x,t) &= p^+ + p^- \\ u(x,t) &= u^+ + u^- , \end{aligned} \tag{16}$$

where $p^+ \overset{\triangle}{=} \mathbf{f}(tI - C_p{}^{-1} X)$, and $\mathbf{f}$ is an arbitrary superposition of right-going components of the form (13) (i.e., taking the minus sign), and $p^- \overset{\triangle}{=} \mathbf{g}(tI + C_p{}^{-1} X)$ is similarly any linear combination of left-going eigensolutions from (13) (all having the plus sign). Similar definitions apply for u^+ and u^-. When the time and space arguments are dropped as in the right-hand side of (16), it is understood that all the quantities are written for the same time t and position x.

When the mass and tension matrices M and K are diagonal, our analysis corresponds to considering m separate waveguides as a whole. For example, the two transversal planes of vibration in a string can be described by (7) with $m = 2$. In a musical instrument such as the piano [29], the coupling among the strings and between different vibration modalities within a single string, occurs primarily at the bridge [30]. Indeed, the bridge acts like a junction of several multivariable waveguides (see section IV).

When the matrices M and K are non-diagonal, the physical interpretation can be of the form

$$C_p{}^2 \overset{\triangle}{=} K M^{-1} , \tag{17}$$

where K is the *stiffness matrix,* and M is the *mass density matrix.* C_p is diagonal if (11) holds, and in this case, the wave equation (7) is decoupled in the spatial dimensions. There are physical examples where the matrices M and K are not diagonal, even though (17) is satisfied with a diagonal C_p. One such example, in the domain of electrical variables, is given by m conductors in a sheath or above a ground plane, where the sheath or the ground plane acts as a coupling element [31, pp. 67–68]. In acoustics, it is more common to have coupling introduced by a dissipative term in equation (7), but the solution can still be expressed as decoupled attenuating traveling waves. An example of such acoustical systems will be presented in Section III-B.

Besides the existence of physical systems that support multivariable traveling wave solutions, there are other practical reasons for considering a multivariable formulation of wave propagation. For instance, modal analysis considers the vector p (whose dimension is infinite in general) of coefficients of the normal mode expansion of the system response. For spaces in perfectly reflecting enclosures, p can be compacted so that each element accounts for all the modes sharing the same spatial dimension [32]. p admits a wave decomposition as in (16), and C_p is diagonal. Having walls with finite impedance, there is a damping term proportional to $\partial p / \partial t$ that functions as a coupling term among the ideal modes [33]. Coupling among the modes can also be exerted by diffusive properties of the enclosure [32], [9].

Note that the multivariable wave equation (7) considered here does not include wave equations governing propagation in multidimensional media (such as membranes, spaces, and solids). In higher dimensions, the solution in the ideal linear lossless case is a superposition of waves traveling in *all directions* in the m-dimensional space [27]. However, it turns out that a good simulation of wave propagation in a multidimensional medium may in fact be obtained by forming a *mesh* of unidirectional waveguides as considered here, each described by (7); such a mesh of 1D waveguides can be shown to solve numerically a discretized wave equation for multidimensional media [34], [35], [13], [14].

3

C. Multivariable Wave Impedance

From (5), we have, using (13),

$$
\begin{aligned}
\partial \boldsymbol{p}(\boldsymbol{x},t)/\partial \boldsymbol{x} &= -\boldsymbol{M}\partial \boldsymbol{u}(\boldsymbol{x},t)/\partial t \\
\Rightarrow \quad \pm s \boldsymbol{C_p}^{-1}\boldsymbol{p} &= -s\boldsymbol{M}\boldsymbol{u} \\
\Rightarrow \quad \boldsymbol{p} &= \pm \boldsymbol{C_p}\boldsymbol{M}\boldsymbol{u} \\
&= \pm \boldsymbol{K}^{1/2}\boldsymbol{M}^{1/2}\boldsymbol{u} \\
&\triangleq \pm \boldsymbol{R}\boldsymbol{u},
\end{aligned}
\tag{18}
$$

where '+' is for right-going and '−' is for left-going. Thus, following the classical definition for the scalar case, the $m \times m$ *wave impedance* is defined by

$$
\boldsymbol{R} \triangleq \boldsymbol{K}^{1/2}\boldsymbol{M}^{1/2} = \boldsymbol{C_p}\boldsymbol{M} = \boldsymbol{K}\boldsymbol{C_u},
\tag{19}
$$

and we have

$$
\begin{aligned}
\boldsymbol{p}^+ &= \boldsymbol{R}\boldsymbol{u}^+ \\
\boldsymbol{p}^- &= - \boldsymbol{R}\boldsymbol{u}^-.
\end{aligned}
\tag{20}
$$

Thus, the wave impedance $\boldsymbol{R}$ is the factor of proportionality between pressure and velocity in a traveling wave. In the cases governed by the ideal wave equation (7), $\boldsymbol{R}$ is diagonal if and only if the mass matrix $\boldsymbol{M}$ is diagonal (since $\boldsymbol{C_p}$ is assumed diagonal). The minus sign for the left-going wave $\boldsymbol{p}^-$ accounts for the fact that velocities must move to the left to generate pressure to the left. The *wave admittance* is defined as $\boldsymbol{\Gamma} = \boldsymbol{R}^{-1}$.

A linear propagation medium in the discrete-time case is completely determined by its *wave impedance* $\boldsymbol{R}(z,\boldsymbol{x})$ which, in a generalized formulation, is frequency dependent and spatially varying. Examples of such general cases will be given in the sections that follow. A *waveguide* is defined for purposes of this paper as a length of medium in which the wave impedance is either constant with respect to spatial position $\boldsymbol{x}$, or else it varies smoothly with $\boldsymbol{x}$ in such a way that there is no scattering (as in the conical acoustic tube[2]). For simplicity, we will suppress the possible spatial dependence and write only $\boldsymbol{R}(z)$, which is intended to be an $m \times m$ function of the complex variable z, analytic for $|z| > 1$.

[2]There appear to be no tube shapes supporting exact traveling waves other than cylindrical and conical (or conical wedge, which is a hybrid) [36]. However, the "Salmon horn family" (see, e.g., [27], [37]) characterizes a larger class of *approximate* one-parameter traveling waves. In the cone, the wave equation is solved for pressure $p(x,t)$ using a change of variables $p' = px$, where x is the distance from the apex of the cone, causing the wave equation for the cone pressure to reduce to the cylindrical case [38]. Note that while pressure waves behave simply as non-dispersive traveling waves in cones, the corresponding velocity waves are *dispersive* [38].

The generalized version of (20) is

$$
\begin{aligned}
\boldsymbol{p}^+ &= \boldsymbol{R}(z)\boldsymbol{u}^+ \\
\boldsymbol{p}^- &= - \boldsymbol{R}^*(1/z^*)\boldsymbol{u}^-
\end{aligned}
\tag{21}
$$

where $\boldsymbol{R}^*(1/z^*)$ is the paraconjugate of $\boldsymbol{R}(z)$, i.e., the unique analytic continuation (when it exists) from the unit circle to the complex plane of the conjugate transposed of $\boldsymbol{R}(z)$ [39].

D. Multivariable Complex Signal Power

The *net complex power* involved in the propagation can be defined as [40]

$$
\begin{aligned}
P &= \boldsymbol{u}^*\boldsymbol{p} = (\boldsymbol{u}^+ + \boldsymbol{u}^-)^*(\boldsymbol{p}^+ + \boldsymbol{p}^-) \\
&= \boldsymbol{u}^{+*}\boldsymbol{R}\boldsymbol{u}^+ - \boldsymbol{u}^{-*}\boldsymbol{R}^*\boldsymbol{u}^- + \\
&\quad \boldsymbol{u}^{-*}\boldsymbol{R}\boldsymbol{u}^+ - \boldsymbol{u}^{+*}\boldsymbol{R}^*\boldsymbol{u}^- \\
&\triangleq (P^+ - P^-) + (P^\times - P^{\times *}),
\end{aligned}
\tag{22}
$$

where all quantities above are functions of z as in (21). The quantity $P^+ = \boldsymbol{u}^{+*}\boldsymbol{R}\boldsymbol{u}^+$ is called *right-going active power* (or right-going average dissipated power[3]), while $P^- = \boldsymbol{u}^{-*}\boldsymbol{R}^*\boldsymbol{u}^-$ is called the *left-going active power*. The term $P^+ - P^-$, the right-going minus the left-going power components, we call the *net active power*, while the term $P^\times - P^{\times *}$ is *net reactive power*. These names all stem from the case in which the matrix $\boldsymbol{R}(z)$ is positive definite for $|z| \geq 1$. In this case, both the components of the active power are real and positive, the active power itself is real, while the reactive power is purely imaginary.

E. Medium Passivity

Following the classical definition of passivity [40], [41], a medium is said to be *passive* if

$$
\mathrm{Re}\{P^+ + P^-\} \geq 0
\tag{23}
$$

for $|z| \geq 1$. Thus, a sufficient condition for ensuring passivity in a medium is that each traveling active-power component is real and non-negative.

To derive a definition of passivity in terms of the wave impedance, consider a perfectly reflecting interruption in the transmission line, such that $\boldsymbol{u}^- = \boldsymbol{u}^+$.

[3]Note that $|z| = 1$ corresponds to the average physical power at frequency ω, where $z = \exp(j\omega T)$, and the wave variable magnitudes on the unit circle may be interpreted as RMS levels. For $|z| > 1$, we may interpret the power $\boldsymbol{u}^*(1/z^*)\boldsymbol{p}(z)$ as the steady state power obtained when exponential damping is introduced into the waveguide giving decay time-constant τ, where $z = \exp(-T/\tau)\exp(j\omega T)$ (for the continuous-time case, see [40, p. 48]).

For a passive medium, using (22), the inequality (23) becomes

$$\boldsymbol{R}(z) + \boldsymbol{R}^*(1/z^*) \geq 0 \qquad (24)$$

for $|z| \geq 1$. I.e., the sum of the wave impedance and its paraconjugate is positive semidefinite.

The wave impedance $\boldsymbol{R}(z)$ is an m-by-m function of the complex variable z. Condition (24) is essentially the same thing as saying $\boldsymbol{R}(z)$ is *positive real*[4] [42], except that it is allowed to be complex, even for real z.

The matrix $\boldsymbol{R}^*(1/z^*)$ is the paraconjugate of $\boldsymbol{R}$. Since $\boldsymbol{R}^*(1/z^*)$ generalizes $\overline{\boldsymbol{R}(e^{j\omega})}^T$, to the entire complex plane, we may interpret $[\boldsymbol{R}(z) + \boldsymbol{R}^*(1/z^*)]/2$ as generalizing the Hermitian part of $\boldsymbol{R}(z)$ to the z-plane, viz., the *para-Hermitian part*.

Since the inverse of a positive-real function is positive real, the corresponding generalized wave admittance $\boldsymbol{\Gamma}(z) = \boldsymbol{R}^{-1}(z)$ is positive real (and hence analytic) in $|z| \geq 1$.

We say that wave propagation in the medium is *lossless* if the impedance matrix is such that

$$\boldsymbol{R}(z) = \boldsymbol{R}^*(1/z^*) \qquad (25)$$

i.e., if $\boldsymbol{R}(z)$ is para-Hermitian (which implies its inverse $\boldsymbol{\Gamma}(z)$ is also).

Most applications in waveguide modeling are concerned with nearly lossless propagation in passive media. In this paper, we will state results for $\boldsymbol{R}(z)$ in the more general case when applicable, while considering applications only for constant and diagonal impedance matrices $\boldsymbol{R}$. As shown in Section II-C, coupling in the wave equation (7) implies a non-diagonal impedance matrix, since there is usually a proportionality between the speed of propagation $\boldsymbol{C_p}$ and the impedance $\boldsymbol{R}$ through the non-diagonal matrix $\boldsymbol{M}$ (see eq. 19).

F. Multivariable Digital Waveguides

The wave components of equations (16) travel undisturbed along each axis. This propagation is implemented digitally using m bidirectional delay lines, as depicted in Fig. 1. We call such a collection of delay lines an *m-variable waveguide section*. Waveguide sections are then joined at their endpoints via scattering junctions (discussed in section IV) to form a DWN.

[4]A complex-valued function of a complex variable $f(z)$ is said to be *positive real* if
1) z real $\Rightarrow f(z)$ real
2) $|z| \geq 1 \Rightarrow \mathrm{Re}\{f(z)\} \geq 0$
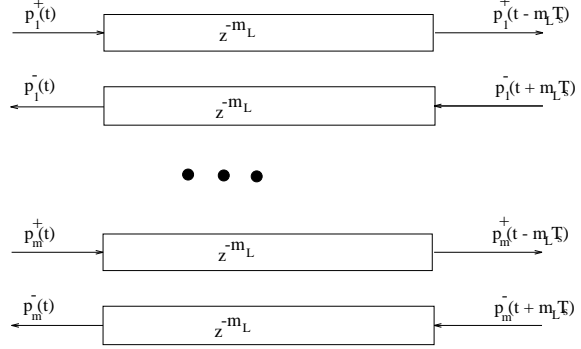Positive real functions characterize passive impedances in classical network theory.

Fig. 1

AN m-VARIABLE WAVEGUIDE SECTION.

III. Lossy Waveguides

A. Multivariable Formulation

The m-variable lossy wave equation is

$$\frac{\partial^2 \boldsymbol{p}(\boldsymbol{x},t)}{\partial t^2} + \boldsymbol{K}\boldsymbol{M}^{-1}\boldsymbol{\Phi}\boldsymbol{K}^{-1}\frac{\partial \boldsymbol{p}(\boldsymbol{x},t)}{\partial t} = \boldsymbol{K}\boldsymbol{M}^{-1}\frac{\partial^2 \boldsymbol{p}(\boldsymbol{x},t)}{\partial \boldsymbol{x}^2} , \qquad (26)$$

where $\boldsymbol{\Phi}$ is a $m \times m$ matrix that represents a viscous resistance. If we plug the eigensolution (10) into (26), we get, in the Laplace domain

$$s^2\boldsymbol{I} + s\boldsymbol{K}\boldsymbol{M}^{-1}\boldsymbol{\Phi}\boldsymbol{K}^{-1} = \boldsymbol{K}\boldsymbol{M}^{-1}\boldsymbol{V}^2 \stackrel{\triangle}{=} \boldsymbol{C_p}^2\boldsymbol{V}^2 \quad (27)$$

or, by letting

$$\boldsymbol{\Phi}\boldsymbol{K}^{-1} \stackrel{\triangle}{=} \boldsymbol{\Upsilon} , \qquad (28)$$

we get

$$s^2\boldsymbol{I} + s\boldsymbol{C_p}^2\boldsymbol{\Upsilon} = \boldsymbol{C_p}^2\boldsymbol{V}^2 . \qquad (29)$$

By restricting the Laplace analysis to the imaginary (frequency) axis $s = j\omega_s$, decomposing the (diagonal) spatial frequency matrix into its real and imaginary parts $\boldsymbol{V} = \boldsymbol{V}_R + j\boldsymbol{V}_I$, and equating the real and imaginary parts of equation (29), we get the equations

$$\boldsymbol{V}_R{}^2 - \boldsymbol{V}_I{}^2 = -\boldsymbol{C_p}^{-2}\omega_s \qquad (30)$$

$$2\boldsymbol{V}_R\boldsymbol{V}_I = \omega_s\boldsymbol{\Upsilon} . \qquad (31)$$

The term $\boldsymbol{V}_R$ can be interpreted as attenuation per unit length, while $\boldsymbol{V}_I$ keeps the role of spatial frequency, so that the traveling wave solution is

$$\boldsymbol{p} = e^{\boldsymbol{V}_R\boldsymbol{X}}e^{j(\omega_s t\boldsymbol{I} - \boldsymbol{V}_I\boldsymbol{X})} \cdot \boldsymbol{1} . \qquad (32)$$

Defining $\boldsymbol{\Theta}$ as the ratio[5] between the real and imaginary parts of $\boldsymbol{V}$ ($\boldsymbol{\Theta}\boldsymbol{V}_I = \boldsymbol{V}_R$), the equations (30)

[5]Indeed, in the general case $\boldsymbol{\Theta}$ is a diagonal matrix.

and (31) become

$$V_I^2 = \left(I - \Theta^2\right)^{-1} \omega_s{}^2 C_p{}^{-2} \qquad (33)$$

$$\Upsilon = 2\Theta \left(I - \Theta^2\right)^{-1} \omega_s C_p{}^{-2} . \qquad (34)$$

Following steps analogous to those of eq. (18), the $m \times m$ admittance matrix turns out to be

$$\Gamma = M^{-1} \left(I - \Theta^2\right)^{-1/2} C_p{}^{-1} - \frac{1}{s} M^{-1} V_R , \quad (35)$$

which, for $\Phi \to 0$, collapses to the reciprocal of (19). For the discrete-time case, we may map $\Gamma(s, \boldsymbol{x})$ from the s plane to the z plane via the bilinear transformation [43], or we may sample the inverse Laplace transform of $\Gamma(s, \boldsymbol{x})$ and take its z transform to obtain $\hat{\Gamma}(z, \boldsymbol{x})$.

B. Example in Acoustics

There are examples of acoustics systems, made of two or more tightly coupled media, whose wave propagation can be simulated by a multivariable waveguide section. One such system is an elastic, porous solid [28, pp. 609–611], where the coupling between gas and solid is given by the frictional force arising when the velocities in the two media are not equal. The wave equation for this acoustic system is (26), where the matrix Φ takes form

$$\Phi = \begin{bmatrix} \Phi & -\Phi \\ -\Phi & \Phi \end{bmatrix} , \qquad (36)$$

and Φ is a flow resistance. The stiffness and the mass matrices are diagonal and can be written as

$$K = \begin{bmatrix} k_a & 0 \\ 0 & k_b \end{bmatrix} ; \qquad (37)$$

$$M = \begin{bmatrix} \mu_a & 0 \\ 0 & \mu_b \end{bmatrix} . \qquad (38)$$

Let us try to enforce a traveling wave solution with spatial and temporal frequencies V and ω_s, respectively:

$$p = p_0 e^{j(Vx - \omega_s t)} = \begin{bmatrix} p_a \\ p_s \end{bmatrix} , \qquad (39)$$

where p_a and p_s are the pressure wave components in the gas and in the solid, respectively. We easily obtain from (26) the two relations

$$j\omega_s \Phi k_s{}^{-1} p_s = (\omega_s{}^2 \alpha_a{}^2 - V^2) p_a \qquad (40)$$

$$j\omega_s \Phi k_a{}^{-1} p_a = (\omega_s{}^2 \alpha_s{}^2 - V^2) p_s , \qquad (41)$$

where

$$\alpha_a{}^2 = c_a{}^{-2} + j \frac{k_s \Phi}{\omega} \qquad (42)$$

$$\alpha_s{}^2 = c_s{}^{-2} + j \frac{k_a \Phi}{\omega} \qquad (43)$$

and c_a and c_s are the sound speeds in the gas and in the solid, respectively. By multiplying together both members of (40) and (41) we get

$$\begin{aligned} V^2 = & \tfrac{1}{2}\omega_s{}^2(\alpha_a{}^2 + \alpha_s{}^2)\pm \\ & \tfrac{1}{2}\sqrt{\omega_s{}^4(\alpha_a{}^2 - \alpha_s{}^2)^2 - 4\omega_s{}^2\Phi^2 k_a k_b}. \end{aligned} \qquad (44)$$

Equation (44) gives us a couple of complex numbers for v, i.e., two attenuating traveling waves forming a vector $\boldsymbol{p}$ as in (32). It can be shown [28, p. 611] that, in the case of small flow resistance, the faster wave propagates at a speed slightly slower than c_s, and the slower wave propagates at a speed slightly faster than c_a. It is also possible to show that the admitance matrix (35) is non-diagonal and frequency dependent.

This example is illustrative of cases in which the matrices K and M are diagonal, and the coupling among different media is exerted via the resistance matrix Φ. If Φ approaches zero, we are back to the case of decoupled waveguides. In any case, two pairs of delay lines are adequate to model this kind of system.

C. Lossy Digital Waveguides

Let us now approach the simulation of propagation in lossy media which are represented by equation (26). We treat the one-dimensional scalar case here in order to focus on the kinds of filters that should be designed to embed losses in digital waveguide networks [44], [25].

As usual, by inserting the exponential eigensolution into the wave equation, we get the one-variable version of (29)

$$\frac{s^2}{c^2} + s\Upsilon = V^2 \qquad (45)$$

where V is the wave number, or spatial frequency, and it represents the wave length and attenuation in the direction of propagation.

Reconsidering the treatment of section III-A and reducing it to the scalar case, let us derive from (33) and (34) the expression for Θ

$$\Theta = \frac{1}{2} \Upsilon \omega_s |V_I|^{-2} , \qquad (46)$$

which gives the unique solution for (33)

$$\Theta = -\frac{\omega_s}{\Upsilon c^2} + \sqrt{\frac{\omega_s{}^2}{\Upsilon^2 c^4} + 1} \; . \qquad (47)$$

This shows us that the exponential attenuation in (32) is frequency dependent, and we can even plot the real and imaginary parts of the wave number V as functions of frequency, as reported in Fig. 2.
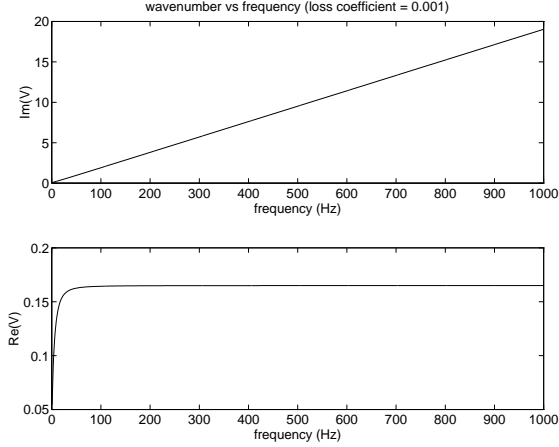

Fig. 2

IMAGINARY AND REAL PART OF THE WAVE NUMBER AS FUNCTIONS OF FREQUENCY ($\Upsilon = 0.001$)

If the frequency range of interest is above a certain threshold, i.e., $\Upsilon c^2/\omega_s$ is small, we can obtain the following relations from (47), by means of a Taylor expansion truncated at the first term:

$$\begin{cases} |v_I| \simeq \frac{\omega_s}{c} \\ |v_R| \simeq \frac{1}{2}\Upsilon c \, . \end{cases} \qquad (48)$$

Namely, for sufficiently high frequencies, the attenuation can be considered to be constant and the dispersion relation can be considered to be the same as in a non-dissipative medium, as it can be seen from Fig. 2.

Still under the assumption of small losses, and truncating the Taylor expansion of Θ to the first term, we find that the wave admittance (35) reduces to the two "directional admittances":

$$\begin{aligned} \Gamma^+ &\triangleq \Gamma(s) = \frac{u^+}{p^+} = G_0\left(1 + \frac{1}{sL}\right) \\ \Gamma^- &\triangleq -\Gamma^*(-s^*) = \frac{u^-}{p^-} = G_0\left(-1 + \frac{1}{sL}\right) \, , \end{aligned} \qquad (49)$$

where $G_0 = \frac{1}{\mu c}$ is the admittance of the medium without losses, and $L = -\frac{2}{\Upsilon c^2}$ is a negative shunt reactance that accounts for losses.

The actual wave admittance of a one-dimensional medium, such as a tube, is $\Gamma(s)$ while $\Gamma^*(-s^*)$ is its paraconjugate in the analog domain. Moving to the discrete-time domain by means of a bilinear transformation, it is easy to verify that we get a couple of "directional admittances" that are related through (21).

In the case of the dissipative tube, as we expect, wave propagation is not lossless, since $R(s) \neq R^*(-s^*)$. However, the medium is passive in the sense of section II-E, since the sum $R(s) + R^*(-s^*)$ is positive semidefinite along the imaginary axis.

The relations here reported hold for any one-dimensional resonator with frictional losses. Therefore, they hold for a certain class of dissipative strings and tubes. Remarkably similar wave admittances are also found for spherical waves propagating in conical tubes (see Appendix A).

The simulation of a length-L_R section of lossy resonator can proceed according to two stages of approximation. If the losses are small (i.e., $\Upsilon \approx 0$) the approximation (48) can be considered valid in all the frequency range of interest. In such case, we can lump all the losses of the section in a single coefficient $g_L = e^{\frac{1}{2}\Upsilon c L_R}$. The resonator can be simulated by the structure of Fig. 3, where we have assumed that the length L_R is equal to an integer number m_L of spatial samples.
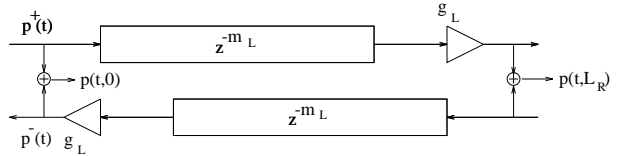

Fig. 3

LENGTH-L_R ONE-VARIABLE WAVEGUIDE SECTION WITH SMALL LOSSES

At a further level of approximation, if the values of Υ are even smaller we can consider the reactive component of the admittance to be zero, thus assuming $\Gamma^+ = \Gamma^- = G_0$.

On the other hand, if losses are significant, we have to represent wave propagation in the two directions with a filter whose frequency response can be deduced from Fig. 2. In practice, we have to insert a filter G_L having magnitude and phase delay that are represented in Fig. 4 for different values of Υ. From such filter we can subtract a contribution of linear phase, which can be implemented by means of a pure delay.
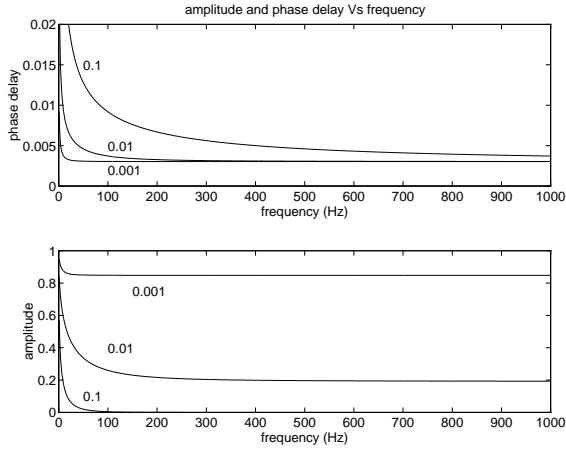
Fig. 4

MAGNITUDE AND PHASE DELAY INTRODUCED BY FRICTIONAL LOSSES IN A WAVEGUIDE SECTION OF LENGTH $L_R = 1$, FOR DIFFERENT VALUES OF Υ
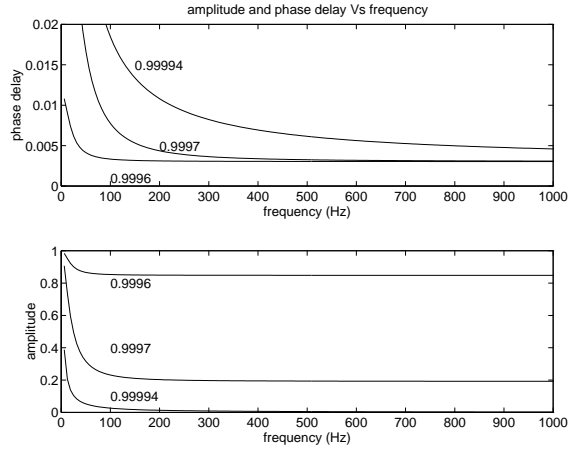

Fig. 5

MAGNITUDE AND PHASE DELAY OF A FIRST-ORDER IIR FILTER, FOR DIFFERENT VALUES OF THE COEFFICIENT r, α IS SET TO $1 - e^{-\frac{1}{2}\Upsilon c L_R}$ WITH THE SAME VALUES OF Υ USED FOR THE CURVES IN FIG. 4

C.1 An Efficient Class of Loss Filters

A first-order IIR filter that, when cascaded with a delay line, simulates wave propagation in a lossy resonator of length L_R, can take the form

$$
\begin{aligned}
G_L(z) &= \left(\alpha \frac{1-r}{1-rz^{-1}} + (1-\alpha) \right) z^{-L_R F_s / c} \\
&\triangleq H_L(z) z^{-L_R F_s / c} .
\end{aligned}
\tag{50}
$$

At the Nyquist frequency, and for $r \simeq 1$, such filter gains $G_L(e^{j\pi}) \simeq 1 - \alpha$ and we have to use $\alpha = 1 - e^{-\frac{1}{2}\Upsilon c L_R}$ to have the correct attenuation at high frequency. Fig. 5 shows the magnitude and phase delay (in seconds) obtained with the first-order filter G_L for three values of its parameter r.

By comparison of the curves of Fig. 4 with the responses of Fig. 5, we see how the latter can be used to represent the losses in a section of one-dimensional waveguide section. Therefore, the simulation scheme turns out to be that of Fig. 6. Of course, better approximations of the curves of Fig. 4 can be obtained by increasing the filter order or, at least, by controlling the zero position of a first-order filter. However, the form (50) is particularly attractive because its low-frequency behavior is controlled by the single parameter r.

As far as the wave impedance is concerned, in the discrete-time domain, it can be represented by a digital filter obtained from (49) by bilinear transforma-
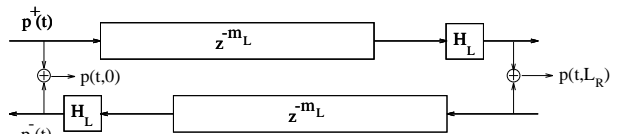

Fig. 6

LENGTH-L_R ONE-VARIABLE WAVEGUIDE SECTION WITH SMALL LOSSES

tion, which leads to

$$
R^+ = \frac{2LF_s}{G_0} \frac{1 - z^{-1}}{2LF_s + 1 - (2LF_s - 1)z^{-1}} ,
\tag{51}
$$

that is a first-order high-pass filter. The discretization by impulse invariance can not be applied in this case because the impedance has a high-frequency response that would alias heavily.

C.2 Validity of Small-Loss Approximation

One might ask how accurate are the small-loss approximations leading to (48). We can give a quantitative answer by considering the knee of the curve in Fig. 4, and saying that we are in the small-losses case if the knee is lower than the lowest modal frequency of the resonator. Given a certain value of friction Υ, we can find the best approximating IIR filter and then find its knee frequency ω_k, corresponding to a magnitude that is $1 + d$ times the asymptotic value,

with d a small positive number. If such frequency ω_k is smaller than the lowest modal frequency we can take the small-losses assumption as valid and use the scheme of fig 3.

C.3 Frequency-Dependent Friction

With a further generalization, we can consider losses that are dependent on frequency, so that the friction coefficient Υ is replaced by $\Upsilon(\omega_s)$. In such case, all the formulas up to (49) will be recomputed with this new $\Upsilon(\omega_s)$.

Quite often, losses are deduced from experimental data which give the value $V_R(\omega_s)$. In these cases, it is useful to calculate the value of $\Upsilon(\omega_s)$ so that the wave admittance can be computed. From (33) we find

$$\Theta = \frac{|V_R|}{\sqrt{\frac{\omega_s^2}{c^2} + V_R{}^2}} \tag{52}$$

and, therefore, from (46) we get

$$\Upsilon(\omega_s) = \frac{2|V_R(\omega_s)|}{\omega_s}\sqrt{\frac{\omega_s^2}{c^2} + V_R(\omega_s)^2}\,. \tag{53}$$

For instance, in a radius-a cylindrical tube, the visco-thermal losses can be approximated by the formula [45]

$$|V_R(\omega_s)| = \frac{3.0 \times 10^{-5}}{a}\sqrt{\frac{\omega_s}{2\pi}}\,, \tag{54}$$

which can be directly replaced into (53).

In vibrating strings, the viscous friction with air determines a damping that can be represented by the formula [45]

$$|V_R(\omega_s)| = a_1\sqrt{\frac{\omega_s}{2\pi}} + a_2\,, \tag{55}$$

where a_1 and a_2 are coefficients that depend on radius and density of the string.

IV. Multivariable Waveguide Junctions

A set of N waveguides can be joined together at one of their endpoints to create an N-port *waveguide junction*. General conditions for lossless scattering in the scalar case appeared in [9]. Waveguide junctions are isomorphic to *adaptors* as used in wave digital filters [22].

This section focuses on physically realizable scattering junctions produced by connecting multivariable waveguides having potentially complex wave impedances. A physical junction can be realized as a parallel connection of waveguides (as in the connection of N tubes that share the same value of pressure at one point), or as a series connection (as in the connection of N strings that share the same value of velocity at one point). The two kinds of junctions are duals of each other, and the resulting matrices share the same structure, exchanging impedance and admittance. Therefore, we only treat the parallel junction.

A. Parallel Junction of Multivariable Complex Waveguides

We now consider the scattering matrix for the parallel junction of N m-variable physical waveguides, and at the same time, we treat the generalized case of matrix transfer-function wave impedances. Equations (21) and (16) can be rewritten for each m-variable branch as

$$\begin{aligned} \boldsymbol{u}_i^+ &= \boldsymbol{\Gamma}_i(z)\boldsymbol{p}_i^+ \\ \boldsymbol{u}_i^- &= -\boldsymbol{\Gamma}_i^*(1/z^*)\boldsymbol{p}_i^-\,, \end{aligned} \tag{56}$$

and

$$\begin{aligned} \boldsymbol{u}_i &= \boldsymbol{u}_i^+ + \boldsymbol{u}_i^- \\ \boldsymbol{p}_i &= \boldsymbol{p}_i^+ + \boldsymbol{p}_i^- = p_{\mathrm{J}}\mathbf{1}\,, \end{aligned} \tag{57}$$

where $\boldsymbol{\Gamma}_i(z) = \boldsymbol{R}_i^{-1}(z)$, p_{J} is the pressure at the junction, and we have used pressure continuity to equate $\boldsymbol{p}_i$ to p_{J} for any i.

Using conservation of velocity we obtain

$$\begin{aligned} 0 &= \mathbf{1}^T\sum_{i=1}^{N}\boldsymbol{u}_i \\ &= \mathbf{1}^T\sum_{i=1}^{N}\left\{\left[\boldsymbol{\Gamma}_i(z) + \boldsymbol{\Gamma}_i^*(1/z^*)\right]\boldsymbol{p}_i^+ \right. \\ &\quad \left. -\boldsymbol{\Gamma}_i^*(1/z^*)p_{\mathrm{J}}\mathbf{1}\right\} \end{aligned} \tag{58}$$

and

$$p_{\mathrm{J}} = S\mathbf{1}^T\sum_{i=1}^{N}\left[\boldsymbol{\Gamma}_i(z) + \boldsymbol{\Gamma}_i^*(1/z^*)\right]\boldsymbol{p}_i^+\,, \tag{59}$$

where

$$S = \left\{\mathbf{1}^T\left[\sum_{i=1}^{N}\boldsymbol{\Gamma}_i^*(1/z^*)\right]\mathbf{1}\right\}^{-1}\,. \tag{60}$$

From (57), we have the scattering relation

$$\boldsymbol{p}^- = \begin{bmatrix} \boldsymbol{p}_1^- \\ \vdots \\ \boldsymbol{p}_N^- \end{bmatrix} = \boldsymbol{A}\boldsymbol{p}^+$$

9

$$= \boldsymbol{A} \begin{bmatrix} \boldsymbol{p}_1^+ \\ \vdots \\ \boldsymbol{p}_N^+ \end{bmatrix} = p_{\mathrm{J}} \begin{bmatrix} 1 \\ \vdots \\ 1 \end{bmatrix} - \boldsymbol{p}^+ , \quad (61)$$

where the scattering matrix is deduced from (59):

$$\boldsymbol{A} = S \begin{bmatrix} \mathbf{1}^T \begin{bmatrix} \boldsymbol{\Gamma}_1 + \boldsymbol{\Gamma}_1^* & \dots & \boldsymbol{\Gamma}_N + \boldsymbol{\Gamma}_N^* \end{bmatrix} \\ \dots \\ \mathbf{1}^T \begin{bmatrix} \boldsymbol{\Gamma}_1 + \boldsymbol{\Gamma}_1^* & \dots & \boldsymbol{\Gamma}_N + \boldsymbol{\Gamma}_N^* \end{bmatrix} \end{bmatrix} - \boldsymbol{I} . \tag{62}$$

If the branches do not all have the same dimensionality m, we may still use the expression (62) by letting m be the largest dimensionality and embedding each branch in an m-variable propagation space.

B. Loaded Junctions

In discrete-time modeling of acoustic systems, it is often useful to attach waveguide junctions to external dynamic systems which act as a *load*. We speak in this case of a *loaded junction* [24]. The load is expressed in general by its complex admittance and can be considered a lumped circuit attached to the distributed waveguide network.

To derive the scattering matrix for the loaded parallel junction of N lossless acoustic tubes, the Kirchhoff's node equation is reformulated so that the sum of velocities meeting at the junction equals the exit velocity (instead of zero). For the series junction of transversely vibrating strings, the sum of forces exerted by the strings on the junction is set equal to the force acting on the load (instead of zero).

The load admittance Γ_{L} is regarded as a *lumped driving-point admittance* [42], and the equation

$$U_{\mathrm{L}}(z) = \Gamma_{\mathrm{L}}(z) p_{\mathrm{J}}(z) \tag{63}$$

expresses the relation at the load.

For the general case of N m-variable physical waveguides, the expression of the scattering matrix is that of (62), with

$$S = \left[\mathbf{1}^T \left(\sum_{i=1}^{N} \boldsymbol{\Gamma}_i \right) \mathbf{1} + \Gamma_{\mathrm{L}} \right]^{-1} . \tag{64}$$

C. Example in Acoustics

As an application of the theory developed herein, we outline the digital simulation of two pairs of piano strings. The strings are attached to a common bridge, which acts as a coupling element between them (see Fig. 7). An in-depth treatment of coupled strings can be found in [30].

To a first approximation, the bridge can be modeled as a lumped mass-spring-damper system, while for the strings, a distributed representation as waveguides is more appropriate. For the purpose of illustrating the theory in its general form, we represent each pair of strings as a single 2-variable waveguide. This approach is justified if we associate the pair with the same key in such a way that both the strings are subject to the same excitation. Actually, the 2×2 matrices $\boldsymbol{M}$ and $\boldsymbol{T}$ of (7) can be considered to be diagonal in this case, thus allowing a description of the system as four separate scalar waveguides.

Fig. 7
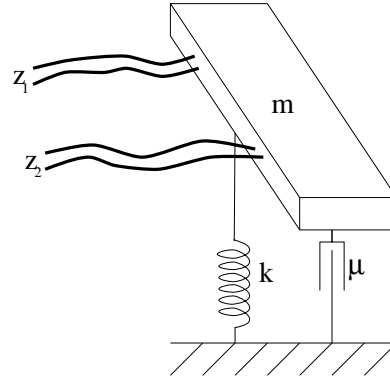TWO PAIRS OF STRINGS COUPLED AT A BRIDGE.

The ith pair of strings is described by the 2-variable impedance matrix

$$\boldsymbol{R}_i = \begin{bmatrix} R_{i,1} & 0 \\ 0 & R_{i,2} \end{bmatrix} . \tag{65}$$

The lumped elements forming the bridge are connected in series, so that the driving-point velocity[6] u is the same for the spring, mass, and damper:

$$u(t) = u_m(t) = u_k(t) = u_\mu(t) . \tag{66}$$

Also, the forces provided by the spring, mass, and damper, add:

$$p(t) = p_m(t) + p_k(t) + p_\mu(t) . \tag{67}$$

We can derive an expression for the bridge impedances using the following relations in the

---

[6]The symbols for the variables velocity and force have been chosen to maintain consistency with the analogous acoustical quantities.

Laplace-transform domain:

$$\begin{aligned}
P_k(s) &= (k/s)U_k(s) \\
P_m(s) &= ms U_m(s) \\
P_\mu(s) &= \mu U_\mu(s) \,.
\end{aligned} \qquad (68)$$

Equations (68) and (67) give the continuous-time load impedance

$$R_{\mathrm{L}}(s) = \frac{P(s)}{U(s)} = m\frac{s^2 + s\mu/m + k/m}{s} \,. \qquad (69)$$

In order to move to the discrete-time domain, we may apply the bilinear transform

$$s \leftarrow \alpha\frac{1 - z^{-1}}{1 + z^{-1}} \qquad (70)$$

to (69). The factor α is used to control the compression of the frequency axis. It may be set to $2/T$ so that the discrete-time filter corresponds to integrating the analog differential equation using the trapezoidal rule, or it may be chosen to preserve the resonance frequency.

We obtain

$$\begin{aligned}
R_{\mathrm{L}}(z) &= & \left[(\alpha^2 - \alpha\mu/m + k/m)z^{-2} \right. \\
&& + \ (-2\alpha^2 + 2k/m)z^{-1} \\
&& + \ \left. (\alpha^2 + \alpha\mu/m + k/m) \right] / \left[\alpha/m(1 - z^{-2}) \right] \,.
\end{aligned}$$

The factor S in the impedance formulation of the scattering matrix (62) is given by

$$S(z) = \left[\sum_{i,j=1}^{2} R_{i,j} + R_{\mathrm{L}}(z) \right]^{-1} , \qquad (71)$$

which is a rational function of the complex variable z. The scattering matrix is given by

$$\boldsymbol{A} = 2S \begin{bmatrix} R_{1,1} & R_{1,2} & R_{2,1} & R_{2,2} \\ R_{1,1} & R_{1,2} & R_{2,1} & R_{2,2} \\ R_{1,1} & R_{1,2} & R_{2,1} & R_{2,2} \\ R_{1,1} & R_{1,2} & R_{2,1} & R_{2,2} \end{bmatrix} - \boldsymbol{I}, \qquad (72)$$

which can be implemented using a single second-order filter having transfer function (71).

V. Conclusions

We presented a generalized formulation of digital waveguide networks derived from a vectorized set of telegrapher's equations. Multivariable complex power was defined, and conditions for "medium passivity" were presented. Incorporation of losses was carried out, and applications were discussed. An efficient class of loss-modeling filters was derived, and a rule for checking validity of the small-loss assumption was proposed. Finally, the form of the scattering matrix was derived in the case of a junction of multivariable waveguides, and an example in musical acoustics was given.

Appendix

I. Propagation of Spherical Waves (Conical Tubes)

We have seen how a tract of cylindrical tube is governed by a partial differential equation such as (7) and, therefore, it admits exact simulation by means of a waveguide section. When the tube has a conical profile, the wave equation is no longer (1), but we can use the equation for propagation of spherical waves [27]:

$$\frac{1}{r^2}\frac{\partial}{\partial r}\left(r^2\frac{\partial p(r,t)}{\partial r} \right) = \frac{1}{c^2}\frac{\partial^2 p(r,t)}{\partial t^2} \,, \qquad (73)$$

where r is the distance from the cone apex.

In the equation (73) we can evidentiate a term in the first derivative, thus obtaining

$$\frac{\partial^2 p(r,t)}{\partial r^2} + \frac{2}{r}\frac{\partial p(r,t)}{\partial r} = \frac{1}{c^2}\frac{\partial^2 p(r,t)}{\partial t^2} \,. \qquad (74)$$

If we recall equation (26) for lossy waveguides, we find some similarities. Indeed, we are going to show that, in the scalar case, the media described by (26) and (74) have structurally similar wave admittances.

Let us put a complex exponential eigensolution in (73), with an amplitude correction that accounts for energy conservation in spherical wavefronts. Since the area of such wavefront is proportional to r^2, such amplitude correction has to be inversely proportional to r, in such a way that the product intensity (that is the square of amplitude) by area is constant. The eigensolution is

$$p(r,t) = \frac{1}{r}e^{st+vr} \,, \qquad (75)$$

where s is the complex temporal frequency, and v is the complex spatial frequency. By substitution of (75) in (73) we find the algebraic relation

$$v = \pm\frac{s}{c} \,. \qquad (76)$$

So, even in this case the pressure can be expressed by the first of (4), where

$$p^+ = \tfrac{1}{r}e^{s(t-r/c)}; \quad p^- = \tfrac{1}{r}e^{s(t+r/c)} \,. \qquad (77)$$

11

Newton's second law

$$\frac{\partial u_r}{\partial t} = -\frac{1}{\rho}\frac{\partial p}{\partial r} \qquad (78)$$

applied to (77) allows to express the particle velocity u_r as

$$u_r(r,t) = \left(\frac{1}{rs} \mp \frac{1}{c}\right)\frac{1}{\rho r}e^{s(t\pm r/c)} . \qquad (79)$$

Therefore, the two wave components of the air flow are given by

$$\begin{array}{l} u^+ = S\left(\frac{1}{rs}+\frac{1}{c}\right)\frac{1}{\rho r}e^{s(t-r/c)} \\ u^- = S\left(\frac{1}{rs}-\frac{1}{c}\right)\frac{1}{\rho r}e^{s(t+r/c)} \end{array} , \qquad (80)$$

where S is the area of the spherical shell outlined by the cone at point r.

We can define the two wave admittances

$$\begin{array}{l} \Gamma^+ = \Gamma(s) = \frac{u^+}{p^+} = G_0\left(1+\frac{1}{sL}\right) \\ \Gamma^- = -\Gamma^*(-s^*) = \frac{u^-}{p^-} = G_0\left(-1+\frac{1}{sL}\right) \end{array} , \qquad (81)$$

where $G_0 = \frac{S}{\rho c}$ is the admittance in the degenerate case of a null tapering angle, and $L = \frac{r}{c}$ is a shunt reactance accounting for conicity [46]. The wave admittance for the cone is $\Gamma(s)$, and $\Gamma^*(-s^*)$ is its para-conjugate in the analog domain. If we translate the equations into the discrete-time domain by bilinear transformation, we can check the validity of equations (21) for the case of the cone.

Wave propagation in conical ducts is not lossless, since $R(s) \neq R^*(-s^*)$. However, the medium is passive in the sense of section II, since the sum $R(s) + R^*(-s^*)$ is positive semidefinite along the imaginary axis.

As compared to the lossy cylindrical tube, the expression for wave admittance is structurally unchanged, with the only exception of the sign inversion in the shunt inductance. This difference is justified by thinking of the shunt inductance as a representation of the signal that does not propagate along the waveguide. In the case of the lossy tube, such signal is dissipated into heat; in the case of the cone, it fills the shell that is formed by interfacing a planar wavefront with a spherical wavefront.

The discrete-time simulation of a length-L_R cone tract having the (left) narrow end at distance r_0 from the apex is depicted in figure 8.

Fig. 8

ONE-VARIABLE WAVEGUIDE SECTION FOR A LENGTH-L_R CONICAL TRACT

REFERENCES

[1] J. O. Smith, "Efficient simulation of the reed-bore and bow-string mechanisms," in *Proc. 1986 Int. Computer Music Conf., The Hague*, pp. 275–280, Computer Music Association, 1986. Also available in [24].
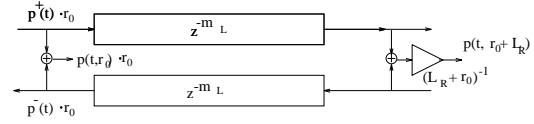
[2] J. O. Smith, "Physical modeling using digital waveguides," *Computer Music J.*, vol. 16, pp. 74–91, Winter 1992. Special issue: Physical Modeling of Musical Instruments, Part I. Available online at http://ccrma.stanford.edu/~jos/.

[3] V. Välimäki and M. Karjalainen, "Improving the Kelly-Lochbaum vocal tract model using conical tube sections and fractional delay filtering techniques," in *Proc. 1994 Int. Conf. Spoken Language Processing (ICSLP-94)*, vol. 2, (Yokohama, Japan), pp. 615–618, IEEE Press, Sept. 18–22 1994.

[4] V. Välimäki, J. Huopaniemi, M. Karjalainen, and Z. Jánosy, "Physical modeling of plucked string instruments with application to real-time sound synthesis," *J. Audio Eng. Soc.*, vol. 44, pp. 331–353, May 1996.

[5] M. Karjalainen, V. Välimäki, and T. Tolonen, "Plucked string models: From the Karplus-Strong algorithm to digital waveguides and beyond," *Computer Music J.*, vol. 22, pp. 17–32, Fall 1998. Available online at http://www.acoustics.hut.fi/~vpv/publications/cmj98.htm.

[6] D. P. Berners, *Acoustics and Signal Processing Techniques for Physical Modeling of Brass Instruments*. PhD thesis, Elec. Eng. Dept., Stanford University (CCRMA), June 1999. Available online at http://ccrma.stanford.edu/~dpberner/.

[7] G. De Poli and D. Rocchesso, "Computational models for musical sound sources," in *Music and Mathematics* (G. Assayag, H. Feichtinger, and J. Rodriguez, eds.), Springer Verlag, 2001. In press.

[8] J. O. Smith, "A new approach to digital reverberation using closed waveguide networks," in *Proc. 1985 Int. Computer Music Conf., Vancouver*, pp. 47–53, Computer Music Association, 1985. Also available in [24].

[9] D. Rocchesso and J. O. Smith, "Circulant and elliptic feedback delay networks for artificial reverberation," *IEEE Trans. Speech and Audio Processing*, vol. 5, no. 1, pp. 51–63, 1997.

[10] D. Rocchesso, "Maximally-diffusive yet efficient feedback delay networks for artificial reverberation," *IEEE Signal Processing Letters*, vol. 4, pp. 252–255, Sept. 1997.

[11] F. Fontana and D. Rocchesso, "Physical modeling of membranes for percussion instruments," *Acustica*, vol. 77, no. 3, pp. 529–542, 1998. S. Hirzel Verlag.

[12] L. Savioja, J. Backman, A. Järvinen, and T. Takala, "Waveguide mesh method for low-frequency simulation of room acoustics," in *Proc. 15th Int. Conf. Acoustics (ICA-95)*, Trondheim, Norway, pp. 637–640, June 1995.

[13] L. Savioja and V. Välimäki, "Reducing the dispersion error in th digital waveguide mesh using interpolation and frequency-warping techniques," *IEEE Trans. Speech and Audio Processing*, vol. 8, pp. 184–194, March 2000.

[14] S. Bilbao, *Wave and Scattering Methods for the Numerical Integration of Partial Differential Equations*. PhD

thesis, Stanford University, June 2001. Available online at http://ccrma.stanford.edu/˜bilbao/.

[15] F. Fontana and D. Rocchesso, "Signal-theoretic characterization of waveguide mesh geometries for models of two-dimensional wave propagation in elastic media," *IEEE Transactions on Speech and Audio Processing*, vol. 9, pp. 152–161, Feb. 2001.

[16] D. T. Murphy and D. M. Howard, "2-D digital waveguide mesh topologies in room acoustics modelling," in *Proc. Conf. Digital Audio Effects (DAFx-00),* Verona, Italy, pp. 211–216, Dec. 2000. Available online at http://www.sci.univr.it/˜dafx/.

[17] P. Huang, S. Serafin, and J. Smith, "A waveguide mesh model of high-frequency violin body resonances," in *Proc. 2000 Int. Computer Music Conf., Berlin*, Aug. 2000.

[18] J. O. Smith, "Principles of digital waveguide models of musical instruments," in *Applications of Digital Signal Processing to Audio and Acoustics* (M. Kahrs and K. Brandenburg, eds.), pp. 417–466, Boston/Dordrecht/London: Kluwer Academic Publishers, 1998. See http://www.wkap.nl/book.htm/0-7923-8130-0.

[19] J. O. Smith and D. Rocchesso, "Aspects of digital waveguide networks for acoustic modeling applications," *http://ccrma.stanford.edu/˜jos/wgj/*, December 19, 1997.

[20] R. J. Anderson and M. W. Spong, "Bilateral control of teleoperators with time delay," *IEEE Trans. Automatic Control*, vol. 34, pp. 494–501, May 1989.

[21] A. Fettweis, "Pseudopassivity, sensitivity, and stability of wave digital filters," *IEEE Trans. Circuit Theory*, vol. 19, pp. 668–673, Nov. 1972.

[22] A. Fettweis, "Wave digital filters: Theory and practice," *Proc. IEEE*, vol. 74, pp. 270–327, Feb. 1986.

[23] J. O. Smith, "Elimination of limit cycles and overflow oscillations in time-varying lattice and ladder digital filters," in *Proc. IEEE Conf. Circuits and Systems, San Jose*, pp. 197–299, May 1986. Conference version. Full version available in [24].

[24] J. O. Smith, "Music applications of digital waveguides," Tech. Rep. STAN–M–39, CCRMA, Music Dept., Stanford University, 1987. A compendium containing four related papers and presentation overheads on digital waveguide reverberation, synthesis, and filtering. CCRMA technical reports can be ordered by calling (650)723-4971 or by sending an email request to info@ccrma.stanford.edu.

[25] D. Rocchesso, *Strutture ed Algoritmi per l'Elaborazione del Suono basati su Reti di Linee di Ritardo Interconnesse*. Phd thesis, Università di Padova, Dipartimento di Elettronica e Informatica, Feb. 1996.

[26] W. C. Elmore and M. A. Heald, *Physics of Waves*. New York: McGraw Hill, 1969. Dover Publ., New York, 1985.

[27] P. M. Morse, *Vibration and Sound*. (516)349-7800 x 481: American Institute of Physics, for the Acoustical Society of America, 1981. 1st ed. 1936, 4th ed. 1981.

[28] P. M. Morse and K. U. Ingard, *Theoretical Acoustics*. New York: McGraw-Hill, 1968.

[29] A. Askenfelt, ed., *Five lectures on the acoustics of the piano*. Stockholm: Royal Swedish Academy of Music, 1990.

[30] G. Weinreich, "Coupled piano strings," *J. Acoustical Soc. of America*, vol. 62, pp. 1474–1484, Dec 1977. Also contained in [29]. See also *Scientific American*, vol. 240, p. 94, 1979.

[31] R. W. Newcomb, *Linear Multiport Synthesis*. New York: McGraw-Hill, 1966.

[32] D. Rocchesso, "The ball within the box: a sound-processing metaphor," *Computer Music J.*, vol. 19, pp. 47–57, Winter 1995.

[33] L. P. Franzoni and E. H. Dowell, "On the accuracy of modal analysis in reverberant acoustical systems with damping," *J. Acoustical Soc. of America*, vol. 97, pp. 687–690, Jan 1995.

[34] S. A. Van Duyne and J. O. Smith, "Physical modeling with the 2-d digital waveguide mesh," in *Proc. International Computer Music Conference*, (Tokyo, Japan), pp. 40–47, ICMA, 1993.

[35] S. A. Van Duyne and J. O. Smith, "The tetrahedral waveguide mesh: Multiply-free computation of wave propagation in free space," in *Proc. IEEE Workshop on Applications of Signal Processing to Audio and Acoustics*, (Mohonk, NY), Oct. 1995.

[36] G. Putland, "Every one-parameter acoustic field obeys webster's horn equation," *J. Audio Eng. Soc.*, vol. 41, pp. 435–451, June 1993.

[37] J. O. Smith, "Waveguide simulation of non-cylindrical acoustic tubes," in *Proc. 1991 Int. Computer Music Conf., Montreal*, pp. 304–307, Computer Music Association, 1991.

[38] R. D. Ayers, L. J. Eliason, and D. Mahgerefteh, "The conical bore in musical acoustics," *American Journal of Physics*, vol. 53, pp. 528–537, June 1985.

[39] P. P. Vaidyanathan, *Multirate Systems and Filter Banks*. Englewood Cliffs, NY: Prentice Hall, 1993.

[40] V. Belevitch, *Classical Network Theory*. San Francisco: Holden-Day, 1968.

[41] M. R. Wohlers, *Lumped and Distributed Passive Networks*. New York: Academic Press, Inc., 1969.

[42] M. E. Van Valkenburg, *Introduction to Modern Network Synthesis*. New York: John Wiley and Sons, Inc., 1960.

[43] T. W. Parks and C. S. Burrus, *Digital Filter Design*. New York: John Wiley and Sons, Inc., June 1987.

[44] N. Amir, G. Rosenhouse, and U. Shimony, "Discrete model for tubular acoustic systems with varying cross section - the direct and inverse problems. Part 1: Theory," *Acta Acustica*, vol. 81, pp. 450–462, 1995.

[45] N. H. Fletcher and T. D. Rossing, *The Physics of Musical Instruments*. New York: Springer-Verlag, 1991.

[46] A. Benade, "Equivalent circuits for conical waveguides," *J. Acoustical Soc. of America*, vol. 83, pp. 1764–1769, May 1988.

Davide Rocchesso is a PhD candidate at the Dipartimento di Elettronica e Informatica, Università di Padova - Italy. He received his Electrical Engineering degree from the Università di Padova in 1992, with a dissertation on real-time physical modeling of music instruments. In 1994 and 1995, he was visiting scholar at the Center for Computer Research in Music and Acoustics (CCRMA), Stanford University. He has been collaborating with the Centro di Sonologia Computazionale (CSC) dell'Università di Padova since 1991, as a researcher and a live-electronic designer/performer. His main interests are in audio signal processing, physical modeling, sound reverberation and spatialization, parallel algorithms. Since 1995 he has been a member of the Board of Directors of the Associazione di Informatica Musicale Italiana (AIMI).
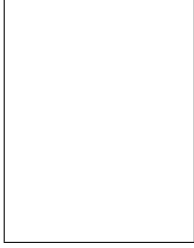
Julius O. Smith received the B.S.E.E. degree from Rice University, Houston, TX, in 1975. He received the M.S. and Ph.D. degrees in E.E. from Stanford University, Stanford, CA, in 1978 and 1983, respectively. His Ph.D. research involved the application of digital signal processing and system identification techniques to the modeling and synthesis of the violin, clarinet, reverberant spaces, and other musical systems. From 1975 to 1977 he worked in the Signal Processing Department at ESL, Sunnyvale, CA, on systems for digital communications. From 1982 to 1986 he was with the Adaptive Systems Department at Systems Control Technology, Palo Alto, CA, where he worked in the areas of adaptive filtering and spectral estimation. From 1986 to 1991 he was employed at NeXT Computer, Inc., responsible for sound, music, and signal processing software for the NeXT computer workstation. Since then he has been an Associate Professor at the Center for Computer Research in Music and Acoustics (CCRMA) at Stanford teaching courses in signal processing and music technology, and pursuing research in signal processing techniques applied to music and audio. For more information, see http://ccrma.stanford.edu/~jos/.